Published in final edited form as:
Nature. 2005 June 9; 435(7043): 765–772.

Structural insights into a yeast prion illuminate nucleation and strain diversity

Rajaraman Krishnan and **Susan L. Lindquist***

Abstract

Self-perpetuating changes in the conformations of amyloidogenic proteins play vital roles in normal biology and disease. Despite intense research, amyloid architecture and conformational conversion remain poorly understood. Amyloid conformers of Sup35 are the molecular embodiment of the yeast prion [*PSI*$^+$], which produces heritable changes in phenotype through self-perpetuating changes in protein folding. We determine the nature of Sup35's cooperatively folded amyloid core and use this information to investigate central questions in prion biology. Specific segments of the amyloid core form intermolecular contacts in a 'Head-to-Head', 'Tail-to-Tail' fashion, while the Central Core is sequestered in intramolecular contacts. The "Head" acquires productive interactions first and these nucleate assembly. Variations in the length of the amyloid core and the nature of intermolecular interfaces are the structural basis of distinct prion "strains", which produce variant phenotypes *in vivo*. These findings solve several problems in yeast prion biology and have broad implications for other amyloids.

Prions proteins share an unusual property: they adopt distinct functional and conformational states that self-perpetuate through protein-conformational chain reactions[1–4]. The first known prion, PrP, facilitates the transmission of a fatal neurodegenerative disease in mammals (spongiform encephalopathy) by converting non-prion conformers to the prion state[4,5]. Fungal prions, however, are not generally pathogenic. Instead, they act as protein-only elements of inheritance. Their prion conformers produce new phenotypes, often beneficial phenotypes[3] by changing processes as diverse as translation termination, nitrogen metabolism, and heterokaryon formation[6]. These phenotypes are heritable because mother cells pass prion conformers on to their daughters, perpetuating the cycle of conversion[1]. A neuronal form of CPEB, a protein implicated in long term memory[7], can also switch to a self-perpetuating prion conformation. In this case, switching activates the protein, suggesting that CPEB's self-perpetuating prion conformation functions in the long-term maintenance of synapses[8]. Most proteins form amyloids under the right idiosyncratic conditions[9]. Prion proteins access such states under normal conditions and some have been conserved for hundreds of millions of years[10]. Prions play a much broader role in biology than previously suspected[11–13].

To understand such self-perpetuating conformational changes we investigated [*PSI*$^+$], a highly conserved *S. cerevisiae* prion. [*PSI*$^+$] confers a wide variety of novel phenotypes by facilitating the read-through of nonsense codons[11–13]. Read-through occurs when Sup35, a translation termination factor, is inactivated by conversion to an amyloid with a self-sustaining structure[1,2,6].

Sup35 has three distinct regions[14,15]: C, a GTP-binding domain at the C-terminus; M, a highly charged middle region; and N, a glutamine/asparagine-rich N-terminal region containing

*Corresponding author, Whitehead Institute for Biomedical Research, Phone: 617-258-5184, Fax: 617-258-7226, Email: Lindquist_admin@wi.mit.edu.
Correspondence and requests for materials should be addressed to S.L.L (Lindquist_admin@wi.mit.edu)

Competing interests statement The authors declare that they have no competing financial interests

oligopeptide repeats. C facilitates translation termination; N and M govern prion status. N is essential for converting Sup35 to the prion state *in vivo*[16] and for converting soluble protein into amyloid fibres *in vitro*[17]. M confers solubility in the non-prion state and stabilizes the prion in mitosis and meiosis[18]. When N and M are removed from *C* and fused to the glucocorticoid receptor, they create a new prion that confers a novel hormone-response phenotype on yeast but otherwise recapitulates all the unusual physical and genetic behaviours of [*PSI*$^+$][19].

In vitro, the conversion of natively unfolded NM to β-rich amyloid fibres involves 1) a lag phase, in which part of the protein oligomerizes and converts to an amyloidogenic nucleus, and 2) an assembly phase, in which soluble proteins rapidly associate with mature nuclei and convert to amyloid[17,20–24]. NM can form distinct types of self-perpetuating conformers[17, 25]. These produce distinct phenotypes (prion strains or variants) when used to transform non-prion [*psi*$^-$] cells to the prion [*PSI*$^+$] state [26,27]. Thus, NM amyloids fully embody the prion, biologically and biochemically.

The ß strands in NM fibres run perpendicular to the main axis and are spaced ~ 4.7 Å apart[20,28]. Many residues are known to affect prion maintenance and fibre assembly[29,30]. However do not yet know 1) the arrangement of individual NM molecules in the amyloid fibre, 2) the mechanisms of nucleation and conformational conversion, or 3) the structural basis of prion strains. Here, we capitalized on NM's lack of cysteines to create a large number of single cysteine variants that could be modified with fluorophores and cross-linkers to address these questions.

Results

Cysteine variants behave like wild type NM

We created 37 individual cysteine-substitution mutations throughout NM (Fig. 1a). Each was used to replace the wild-type (WT) *SUP35* gene *in vivo*. All retained the capacity to support the [*PSI*$^+$] and [*psi*$^-$] states (Fig. S1a). None altered the stability of those states (data not shown).

Next, each protein was expressed in and purified from *E.coli.* All spontaneously assembled into amyloid at the same rate as WT (Fig. S1b). Moreover, all fibres were indistinguishable from WT by electron microscopy and SDS (sodium dodecyl sulphate) solubility[22] (data not shown). Finally, fibres made from each mutant seeded assembly as well as WT (Fig. S1c)[17, 20]. Having established that cysteine substitution proteins recapitulate prion behaviour *in vivo* and *in vitro*, we employed them to explore NM structure and assembly.

Boundaries of the cooperatively folded amyloid

We used two independent approaches to investigate the structure of NM fibres. First, in 37 sets of fibres assembled at 25°C from each variant, we probed the accessibility of cysteines to labelling with pyrene maleimide, and to a more hydrophilic reagent, Lucifer Yellow (Fig. 1b and data not shown). Proteins carrying cysteines between amino acid residues (aa) 25–58 were sparsely labelled. Proteins with cysteines between aa 2–21 and 68–112 showed partial accessibility. All cysteines in M were highly accessible.

Next, we used acrylodan to report on the conformational status of different segments of NM. Acrylodan exhibits an increase in fluorescence intensity and a blue shift in λ_{max} when sequestered from solvent. When denatured, all cysteine-labelled proteins had a λ_{max} around 530 nm. After assembly at 25°C, proteins labelled between aa 21–121 had strongly blue-shifted emissions (λ_{max}486–488 nm) indicating sequestration from solvent (Fig. 1c, zero guanidine hydrochloride, GdmCl, and data not shown). Proteins labelled in adjoining regions (residue 7 N-terminally and residues 137, 158 and 167 C-terminally) had partially blue-shifted emission

maxima (λ_{max} 493 to 525 nm). Proteins labelled at 2, 184, 225 and 234 had no significant blue shift, indicating that these residues remained exposed to solvent pre- and post-assembly (Fig. 1c and data not shown).

To determine which residues participate in the same cooperatively folded structure, we assessed their post-assembly GdmCl denaturation profiles, using 24 GdmCl concentrations for each of the fibres. All fibres labelled between aa 21–121 showed a similar drop in fluorescence intensity and a corresponding red shift in emission maxima with an inflection at 2.5M (± 0.15 M) GdmCl (Fig. 1c). These profiles fitted a monophasic unfolding transition that corresponded to the major unfolding transition of WT NM protein (Cashikar and Lindquist, unpublished results). Adjacent cysteine variants with intermediate blue shifts on fibrillization also had distinct unfolding transitions in GdmCl.

These studies establish that: 1) a large portion of N is sequestered from solvent; 2) a sub-portion constitutes a distinct domain (formed by contiguous aa including 21–121) with an unusually stable structure and a single cooperative unfolding transition; 3) flanking sequences are structurally heterogeneous, with residues 137 and 158 having distinct, but cooperative, unfolding transitions and residues 2 and 7 biphasic transitions; and 4) beyond residue 158 M is flexible and solvent exposed. Residues in the N/M transition zone (aa 121, 137 and 158) were fully accessible to cysteine labelling but by acrylodan labelling and GdmCl denaturation were partially sequestered and structured. This likely reflects different sensitivities of the two techniques to structural instability. For example, if residue 121 adopts an open structure occasionally, it would exhibit a strong blue shift with acrylodan, but still be accessible to prolonged labelling.

Identifying intermolecular contacts

To determine which regions of NM make intermolecular contacts in fibres, we exploited the ability of pyrene-labelled proteins to form excimers (excited-state dimers). When two pyrenes lie within 4–10 Å of each other, the long fluorescence lifetime of pyrene allows an excited residue to interact with an unexcited residue before energy is emitted. This produces a strong red shift in fluorescence. Excimer fluorescence will occur between residues at β-strands that form the interface between two monomers (Fig. 2a) but not between residues that are distant from the interface (Fig. 2b). (One caveat is that the pyrenes might alter the structure formed. Control experiments eliminated this concern. See Fig. S2c).

In denaturant each of the pyrene-labelled proteins had multiple emission maxima between 384 and 405 nm (Fig. S2a and S2b). After assembly at 25°C, most proteins labelled in the N region exhibited a blue shift in fluorescence (Fig. S2b), indicating that they were sequestered from intermolecular contacts. Proteins labelled in two distinct regions (residues 25, 31, 38 and 91, 96, 106) produced strong red-shifted fluorescence (λ_{max} ~465 nm; Fig. 2a and Fig. S2a). These residues must lie at or near a contact between two NM molecules. We will refer to these intermolecular contact regions as the “Head” (aa 25–38) and “Tail” (aa 91–106). Residues between them, the “Central Core” (43–85), are also part of the cooperatively folded amyloid but are sequestered from intermolecular contacts.

Pyrene fluorescence patterns were virtually identical in repeat experiments (data not shown). They were also nearly identical in seeded and unseeded-rotated reactions (open and closed circles, Fig. 2a). The remarkable reproducibility of these excimer patterns establishes that the intermolecular contacts in seeded assembly quite precisely recapitulate those of spontaneous assembly.

Next, we mixed proteins labelled at two different cysteines in all pair-wise combinations (Fig. 2b and Fig. S3). Confirming that residues in the Central Core do not contribute to intermolecular

contacts, all fibres in which either one or both of the proteins were labelled in this region produced low excimer signals (residues 51, 58 and 73; Fig. 2b and Fig. S3). The strongest signals were again from the Head and Tail, but only when both proteins were labelled in the same region (Fig. 2b, orange boxes). Fibres with one protein labelled in the Head and another in the Tail produced weak signals. We conclude that contacts between monomers in the fibre occur in a Head-to-Head and Tail-to-Tail fashion.

These data are not compatible with the parallel super-pleated sheet model for the Sup35 prion domain[31], in which individual NM molecules fold into long serpentine arrays, stacked in parallel along their entire length. They are compatible with a ß-helix model[28], and related ß-spiral and ß-sandwich models, wherein a contiguous stretch of amino acids forms the amyloid fold and a Central Core is sequestered from intermolecular contacts. Further, individual subunits must form contacts in a Head-to-Head and Tail-to-Tail fashion (see Fig. 3).

Constraints on inter-subunit relationships

To provide an independent assessment of inter-subunit interactions, we introduced two types of crosslinks into each of the individual cysteine-substituted proteins under denaturing conditions. Reaction with oxidized DTT produced disulfides with a bond length of ~2Å. Reaction with 1, 4-bis-maleimidobutane (BMB), a homobifunctional agent, produced crosslinks with a 10.9Å flexible linker.

Disulfide cross-links inhibited fibre formation at every position tested between aa 21–121 (Fig. 2c, black bars; thioflavinT fluorescence levels equivalent to those of BSA aggregates). Disulfides in the extreme N terminus and in M had little effect on assembly. In contrast, with the flexible BMB linker, NM molecules cross-linked in the Head or Tail formed fibres very efficiently (Fig. 2c, grey bars). BMB cross-links severely impeded fibre formation only in the Central Core.

The ~2Å bond length of a disulfide is closer than the inter-strand distances of ~4.7Å that characterize NM fibres[20,28]. The distributions of residues for which disulfides inhibit amyloid formation support our earlier conclusion that a contiguous linear segment of aas, including aa 21–121, constitute a cooperatively folded unit. Improper intersubunit alignments of any two residues in this region prevent folding of the rest of the domain. The extreme N-terminus and the middle domain are outside this domain and have little influence on its capacity to fold.

With the longer linker, apposition of two NM proteins in the Head or Tail permits fibre formation. Apposition of Central Core residues prevents it. Thus, the separation of Central Core regions is not only a general characteristic of NM fibres but is essential for fibre formation.

Next we asked whether the structural information and the tools we had assembled could be employed to address two of the most enigmatic questions in prion biology. How is assembly nucleated? What is the structural basis of distinct prion strains?

Early events during nucleation and assembly

First, we first monitored kinetic changes in the fluorescence of proteins labelled with acrylodan. All tested proteins labelled in the cooperatively folded amyloid region (21–106) showed a very rapid increase in fluorescence, characteristic of a first-order reaction with no lag phase (Fig. 4a). This fluorescence increase preceded conversion to amyloid: when amyloid formation was monitored by the acquisition of an SDS-insoluble state, each acrylodan-labelled protein had the same lag and assembly phase as WT protein (Fig. S4). In contrast, molecules labelled at residues 158 or 167 changed fluorescence simultaneously with amyloid formation (Fig. 4a and data not shown). Proteins labelled at residue 184, 203, and 225 showed no change in fluorescence (Fig. 4a and data not shown). We conclude that: 1) residues that form the

cooperatively folded amyloid core rapidly enter a collapsed but non-amyloid state, 2) M residues proximal to N become structured only when N residues convert to amyloid, and 3) the distal region of M remains largely unstructured and exposed to solvent after amyloid assembly.

To determine which segments of the cooperatively folded amyloid region are the first to undergo conformational commitment, we took advantage of the fact that disulfide bonds anywhere in this region to prohibit assembly (Fig. 2c). We reasoned that segments of NM that are the first to assume productive spatial relationships would also be the first to be protected from the spontaneous formation of disulfide bonds. Representative cysteine mutants were allowed to assemble in buffer without DTT, to facilitate the formation of disulfide bonds, and analysed on SDS gels without DTT. Cysteines in the Head (21, 25, and 31) formed fewer disulfides than cysteines at other positions (Fig. 4b). Thus, during conformational conversion, strand spacings compatible with a productive fold (and incompatible with disulfide formation) are achieved in the Head region more rapidly than in other regions.

Next, we investigated the effects of adding a single charge at various positions in the amyloid region. In some ß-structures, such as the ß-helix, alternating residues point toward or away from solvent and the structures formed are very stable [32]. Although introduction of a single charge would be unlikely to perturb such structures once they form, charge repulsions in early nucleating segments of the molten, collapsed intermediate would reduce the frequency with which these segments come into proximity and, thereby, slow nucleation. Labelling individual NM cysteine residues with uncharged iodoacetamide had little effect on the quantity of protein converting to amyloid (Fig. 4c) or the kinetics of assembly (Fig. S5). In contrast iodoacetate labelling, which introduces a negatively charged moiety of similar size, inhibited assembly most strongly in the Head region (Fig. 4c and Fig. S5).

Finally, if Head-to-Head interactions are not only characteristic of early productive amyloid conformations, but actually cause a commitment to it, bringing Head regions in proximity with each other should promote nucleation. We compared assembly kinetics for several NM variants that were cross-linked with BMB under denaturing conditions and then transferred to assembly buffer. Crosslinks in the Central Core (aa 43,73) blocked assembly entirely, confirming that these regions must be separated from each other to form amyloid (Fig. 4d). Cross-links in the Tail (96, 106) had little effect. Cross-links in the Head (aa 21,25,38) virtually eliminated the lag phase. Thus, the juxtaposition of residues in the Head region is an early event in amyloid formation and is, indeed, sufficient to nucleate it.

Structural distinctions between prion strain populations

To place the second critical question in prion biology – the basis of prion “strains” or variants – within the structural framework we have generated for NM fibres, we assembled the protein under conditions previously known to produce different strain populations (room temperature, RT, versus 4°C) [32]. We confirmed that fibres produced at 4°C, (1) assembled much more rapidly[26] (data not shown), (2) were less stable to GdmCl denaturation (Fig. 5a), and (3) produced mostly strong prion strains when used to transform cells from the [*psi*$^{-}$] non-prion state to the [*PSI*$^{+}$] prion state (Fig 5c, left) [32].

Do fibres enriched in different prion strains have distinct cooperatively folded amyloid domains? Denaturation profiles of fibres, independently assembled from 16 acrylodan-labelled proteins at either 4°C or 25°C, were determined as in Fig. 1c. In 4°C fibres, residues 31–86 had strong blue shifts in fluorescence upon assembly and exhibited a single cooperative unfolding transition at $D_{½}$ ~ 1.5 M GdmCl, (Fig. 5a and data not shown). Flanking residues 21, 25, 96, 112, and 121, had smaller blue shifts in fluorescence upon assembly and heterogeneous denaturation profiles after assembly, as had residues flanking the 25°C amyloid

domain (2 and 7, 137 and 158; Fig. 1c, Fig 5a, and data not shown). Thus, at both temperatures the cooperatively folded amyloid core has a similar character: it is formed by a contiguous stretch of amino acids and is flanked by residues that are structurally heterogeneous. However, the length of the region incorporated into the cooperative amyloid fold is much shorter in 4°C fibres than in 25°C fibres and, consequently, more easily denatured. Shorter less stable amyloid cores likely produce stronger more stably inherited prion strains because the fibres are more easily fragmented and transmitted to daughter cells.

Finally, we asked if intermolecular contacts differ in fibres assembled at 4°C and 25°C. The excimer fluorescence of residues in the Head region and in flanking residues (2, 7, and 16) changed modestly but in an extremely reproducible manner (seeded and unseeded reactions; Fig. 5b). Excimer fluorescence in the Tail shifted the most dramatically. Thus, as the number of residues that constitute the cooperatively folded amyloid domain change, the intersubunit interfaces change as well.

The Structural basis of prion strains

In fibres enriched for distinct prion strains we confirmed[27] differences in the rate of assembly, and discovered differences in both the length of the amyloid core and intersubunit contacts. But are these features determinative? If so, proteins cross-linked in different places should strongly bias assembly reactions toward different strains.

Proteins cross-linked with BMB (as for Fig. 2c) were assembled at 25°C or 4°C and used to transform cells from the [*psi*$^{-}$] to the [*PSI*$^{+}$] state[26,27]. Proteins cross-linked in the Central Core did not induce [*PSI*$^{+}$] above background levels (Fig. 5c), consistent with their failure to undergo amyloid assembly (Fig 2c). Cross-links in the Head, which caused rapid assembly, biased fibres towards the production of strong strains. Conversely cross-links in the Tail, which should cause a longer segment to be incorporated into the amyloid fold, biased fibres towards weak strains (Fig. 5c). Notably, the strain biases produced by different cross-link positions overcame those of different assembly temperatures. Whether the fibres used for transformation had been assembled at 4°C or at 25°C, proteins cross-linked in the Head produced primarily strong strains and proteins cross-linked in the Tail produced primarily weak strains (Fig. 5d). Thus, strain distinctions are due to differences in the secondary and tertiary structures of individual NM molecules, as well as to the nature of NM::NM interactions.

Discussion

Our results provide a framework for the structure of NM fibres, define rate-limiting events that govern their nucleation and establish a physical basis for prion “strains”. The data provide many insights on prion initiation and propagation and are likely to shed light on amyloid biology in other systems.

The first step in assembly is the formation of a collapsed intermediate in which residues in the N region are sequestered from solvent but have not yet locked into their final structures (Figs. 4a and S4). The search for structure in globular proteins also begins with a collapsed intermediate, but these are dominated by hydrophobic interactions. The N collapse must be governed by polar interactions and/or backbone interactions, since polar residues outweigh hydrophobic residues 16 to 1. Hence, proteins governed by very different interactions, and achieving very different final structures, both do so through a molten collapsed intermediate.

Within this collapsed state, it is the Head region that commits most rapidly to amyloid-compatible spatial relationships (Fig. 4b). Moreover, simply bringing the Head regions of two NM molecules into close proximity triggers nucleation (Fig 4d). We suggest that Head-to-Head contacts are a major route for NM nucleation, funnelling the protein away from other folding

pathways that might still be productive but are much slower. The lag phase of assembly would then represent the time required to search out these productive contacts in the collapsed molten state. The importance of Head-to-Head contacts in nucleation clarifies why the "species barrier", which prevents cross-species seeding between *S. cerevisiae* and *C. albicans* NM proteins, maps to this region [2,33,34].

After nucleation, fibres grow through Head-to-Head and Tail-to-Tail interactions (Figs. 2a,b, and 3). This explains why they grow bi-directionally [21]. Moreover, the fact that both ends of NM are involved in prion propagation explains why rare cross seeding events (between NM proteins from diverse species and between entirely different prions in the same species) rapidly convert from heterotypic to homotypic interactions [35–37]. Once the heterologous protein has joined the fibre, it will immediately present a homotypic interface for either Head-to-Head or Tail-to-Tail interactions.

Our work also sheds light on the crucial role played by the five and a half degenerate oligopeptide repeats (consensus sequence P/QQGGYQQ/SYN). Increasing these repeats greatly increases spontaneous prion formation *in vivo* and fibre nucleation *in vitro* [38]. Reducing them eliminates the protein's ability to propagate as a prion *in vivo* on its own. Yet even a single repeat allows efficient incorporation into pre-existing WT prions [38–40]. We find that most repeats are sequestered from intermolecular contacts in the Central Core (Figs. 2 and 4d), whose length determines fibre stability (Fig 5a). However, intermolecular Tail-to-Tail contacts include the final 1.5 to 2.5 repeats. That is, repeat-to-repeat contacts are accommodated in both intramolecular and intermolecular amyloid interactions. With a single repeat the stability of NM amyloid (for example to the fragmentation activity of Hsp104) might fall below the threshold required to maintain the prion state on its own, but NM could still join pre-existing WT prions, repeat interacting with repeat. Noting that the repeat sequence is able to form an amyloid on its own[41], we further propose that the closely spaced repeat sequences of individual NM molecules readily collapse into transient pre-amyloid structures within the molten intermediates where nucleation occurs. The more repeats, the more likely this transient structure is to form, reducing the number of contacts the Head region must sample to initiate nucleation.

What structural elements are responsible for enciphering prion strains? Previous data are perplexing. On the one hand, amyloids assembled *in vitro* from a fragment containing only the first 65 residues of N can induce a broad spectrum of distinct heritable prion strains when used to transform [*psi*−] cells[26]. On the other hand, during *in vivo* propagation, residues through 137 are required to maintain multiple [*PSI*$^+$] strains [42]. The extremely reproducible pyrene excimer signals in our experiments (Fig 2a and 5b) provide a key. Different intermolecular contacts in both the Head and Tail create distinct strains. The fragment 1–65 contains the Head region and two repeats. It should be able to form the full spectrum of Head region interactions that distinguish different strains and be able to propagate these to WT protein. However, differences in the length of the core and the position of Tail-to-Tail contacts are the major distinctions between prion strains. Hence, this region is required for the maintenance of distinct strains *in vivo*.

Does our data have relevance to other prions and amyloids? Although it is not yet clear that molten oligomeric species are obligate intermediates in the formation of other amyloids (as it is for NM), they are present in the initial stages of many amyloid assemblies [43,44]. Evidence also attests to the importance of dimeric interactions in the assembly of diverse amyloids [45–47]. Enticingly, recent molecular dynamics simulations with Aß peptide suggest assembly begins with a molten oligomeric species that allows the rapid sampling of multiple intermolecular contacts, with two individual molecules precipitously finding the right contact and nucleating assembly[44].

For the mammalian prion determinant, PrP, several other similarities are apparent, including: 1) electron crystallography data supporting a ß helix-like structure in the prion state [48,49]; 2) the importance of PHGGGWGQ oligopeptide repeats (increasing them causes spontaneous prion formation, eliminating them inhibits propagation); and 3) the ability of PrP to form a variety of phenotypically distinct strains with different structures (i.e. different sensitivities to GdmCl denaturation, protease cleavage sites and glycosylation states)[50].

For simplicity, we distinguished only strong and weak strains of NM but, in fact, each category includes a multiplicity of strains (27 and data not shown). We suggest that promiscuities in intermolecular Head and Tail contacts, together with the low sequence complexity of the N domain (72% Q, N, G, and Y) allow differences in intermolecular contacts to ratchet the amyloid core into different registers, creating an ensemble of structures with closely related but distinct ß-strand contacts. If the length of the amyloid core and the residues involved in contact interfaces differ for PrP strains as they do for NM, it would readily explain variations in transmission within and between species. One fold might display an interface that is polymorphic between species, another one that is invariant. One fold might restrict the incorporation of a glycosylated residue because the modified side chain would point inward; another might permit it because the residue points outward. Similarly, transient intramolecular ß-structures formed by expanded oligopeptide repeats would reduce the number of intermolecular contacts sampled to nucleate prion formation, even though the prion-enhancing PrP repeats lie outside the amyloid core[4,5]. There will undoubtedly be many variations in the structure and dynamics of amyloid assemblies, but several of the principles we have uncovered, as well as the methods we employed, will likely be applicable to other systems.

Materials and Methods

Mutagenesis, protein purification and yeast strains

The site-specific substitution of individual amino-acid codons for cysteine codons, the production of integrating genomic constructs, the strategy for replacing *WT* SUP35 with the cysteine mutants, overexpression and purification of cysteine mutants is described in the supplementary materials.

Cysteine labelling

a. Post-assembly: 5uM fibres were incubated with 15μM of pyrene maleimide or 15 uM Lucifer yellow for 3 hours. Fibres were washed thrice with 20% methanol +5 mM DTT and redissolved in 6M GdmCl. Labelling efficiencies were calculated according to Molecular probes URL: www.probes.com.

b. Pre-assembly: proteins were incubated in 6MGdmCl with acrylodan or pyrene maleimide precisely as recommended (URL: www.probes.com). Labelling efficiencies for acrylodan (>90%) and pyrene (70–80%) were also determined according to the manufacturer's protocol.

c. Iodoacetate and iodoacetamide labelling in 6 M GdmCl employed 25μM protein and a 5-fold excess of iodoacetate or iodoacetamide for 2 hours at 25°C. After using a PD10 desalting column (Pharmacia) to remove free label, efficiencies were determined from the number of free thiols still accessible to 5,5′-dithiobis- 2-nitro-benzoic acid.

d. BMB (1, 4-bis-Maleimidobutane) was employed at a protein to reagent ratio of 1:2, O-DTT (oxidized dithiothreitol) at a ratio of 5:1. Reactions in 6M GdmCl were terminated after 3 hours with 5 mM DTT. Cross-linking efficiencies (all between 70–85%) were assessed by SDS-PAGE.

Protein transformation—Yeast cells containing an ADE1 mutation suppressible by [*PSI* +] were co-transformed with NM proteins and a URA3 plasmid as described[27]. Ura+ transformants were picked prior to colour development (three days instead of seven), to avoid bias. Approximately 200 transformants for each mutant, in each case obtained from five independent transformations, were patched onto uracil– media and replica plated to both adenine– media and 25% rich media supplemented with 20μg/ml adenine. Transformation efficiencies were calculated (Fig S6) and strong and weak strains were scored[27] by colour on YPD (see Fig S1) and rates of growth on adenine– medium.

Supplementary Material

Refer to Web version on PubMed Central for supplementary material.

Acknowledgements

We thank Jonathan Weissman for providing us with the fibre transformation protocols, members of the Lindquist, Langen and Berger Labs for helpful discussions and Robert Latek and Tom DiCesare for help with the figures. This research was supported by the DuPont-MIT Alliance and NIH grant GM25874.

References

1. Tuite MF, Cox BS. Propagation of yeast prions. Nat Rev Mol Cell Biol 2003;4:878–90. [PubMed: 14625537]
2. Chien P, Weissman JS, DePace AH. Emerging principles of conformation-based prion inheritance. Annu Rev Biochem 2004;73:617–56. [PubMed: 15189155]
3. Shorter, J. & Lindquist, S. Prions as adaptive conduits of memory and inheritance. *Nature Reviews Genetics***(in press)** (2005).
4. Caughey B. Transmissible spongiform encephalopathies, amyloidoses and yeast prions: common threads? Nat Med 2000;6:751–4. [PubMed: 10888922]
5. Prusiner SB. Prions. Proc Natl Acad Sci U S A 1998;95:13363–83. [PubMed: 9811807]
6. Uptain SM, Lindquist S. Prions as protein-based genetic elements. Annu Rev Microbiol 2002;56:703–41. [PubMed: 12142498]
7. Si K, et al. A neuronal isoform of CPEB regulates local protein synthesis and stabilizes synapse-specific long-term facilitation in aplysia. Cell 2003;115:893–904. [PubMed: 14697206]
8. Si K, Lindquist S, Kandel ER. A neuronal isoform of the aplysia CPEB has prion-like properties. Cell 2003;115:879–91. [PubMed: 14697205]
9. Dobson CM. Protein folding and misfolding. Nature 2003;426:884–90. [PubMed: 14685248]
10. Jensen MA, True HL, Chernoff YO, Lindquist S. Molecular population genetics and evolution of a prion-like protein in Saccharomyces cerevisiae. Genetics 2001;159:527–35. [PubMed: 11606530]
11. Eaglestone SS, Cox BS, Tuite MF. Translation termination efficiency can be regulated in Saccharomyces cerevisiae by environmental stress through a prion-mediated mechanism. Embo J 1999;18:1974–81. [PubMed: 10202160]
12. True HL, Lindquist SL. A yeast prion provides a mechanism for genetic variation and phenotypic diversity. Nature 2000;407:477–83. [PubMed: 11028992]
13. True HL, Berlin I, Lindquist SL. Epigenetic regulation of translation reveals hidden genetic variation to produce complex traits. Nature 2004;431:184–7. [PubMed: 15311209]
14. Kushnirov VV, et al. Divergence and conservation of SUP2 (SUP35) gene of yeast Pichia pinus and Saccharomyces cerevisiae. Yeast 1990;6:461–72. [PubMed: 2080663]
15. Ter-Avanesyan MD, et al. Deletion analysis of the SUP35 gene of the yeast Saccharomyces cerevisiae reveals two non-overlapping functional regions in the encoded protein. Mol Microbiol 1993;7:683–92. [PubMed: 8469113]
16. Chernoff YO, Derkach IL, Inge-Vechtomov SG. Multicopy SUP35 gene induces de-novo appearance of psi-like factors in the yeast Saccharomyces cerevisiae. Curr Genet 1993;24:268–70. [PubMed: 8221937]

17. Glover JR, et al. Self-seeded fibers formed by Sup35, the protein determinant of [PSI+], a heritable prion-like factor of S. cerevisiae. Cell 1997;89:811–9. [PubMed: 9182769]
18. Liu JJ, Sondheimer N, Lindquist SL. Changes in the middle region of Sup35 profoundly alter the nature of epigenetic inheritance for the yeast prion [PSI+]. Proc Natl Acad Sci U S A 2002;99 (Suppl 4):16446–53. [PubMed: 12461168]
19. Li L, Lindquist S. Creating a protein-based element of inheritance. Science 2000;287:661–4. [PubMed: 10650001]
20. Serio TR, et al. Nucleated conformational conversion and the replication of conformational information by a prion determinant. Science 2000;289:1317–21. [PubMed: 10958771]
21. Scheibel T, Kowal AS, Bloom JD, Lindquist SL. Bidirectional amyloid fiber growth for a yeast prion determinant. Curr Biol 2001;11:366–9. [PubMed: 11267875]
22. Scheibel T, Bloom J, Lindquist SL. The elongation of yeast prion fibers involves separable steps of association and conversion. Proc Natl Acad Sci U S A 2004;101:2287–92. [PubMed: 14983002]
23. Shorter J, Lindquist S. Hsp104 catalyzes formation and elimination of self-replicating Sup35 prion conformers. Science 2004;304:1793–7. [PubMed: 15155912]
24. Collins SR, Douglass A, Vale RD, Weissman JS. Mechanism of prion propagation: amyloid growth occurs by monomer addition. PLoS Biol 2004;2:e321. [PubMed: 15383837]
25. DePace AH, Weissman JS. Origins and kinetic consequences of diversity in Sup35 yeast prion fibers. Nat Struct Biol 2002;9:389–96. [PubMed: 11938354]
26. King CY, Diaz-Avalos R. Protein-only transmission of three yeast prion strains. Nature 2004;428:319–23. [PubMed: 15029195]
27. Tanaka M, Chien P, Naber N, Cooke R, Weissman JS. Conformational variations in an infectious protein determine prion strain differences. Nature 2004;428:323–8. [PubMed: 15029196]
28. Kishimoto A, et al. beta-Helix is a likely core structure of yeast prion Sup35 amyloid fibers. Biochem Biophys Res Commun 2004;315:739–45. [PubMed: 14975763]
29. DePace AH, Santoso A, Hillner P, Weissman JS. A critical role for amino-terminal glutamine/asparagine repeats in the formation and propagation of a yeast prion. Cell 1998;93:1241–52. [PubMed: 9657156]
30. King CY. Supporting the structural basis of prion strains: induction and identification of [PSI] variants. J Mol Biol 2001;307:1247–60. [PubMed: 11292339]
31. Kajava AV, Baxa U, Wickner RB, Steven AC. A model for Ure2p prion filaments and other amyloids: the parallel superpleated beta-structure. Proc Natl Acad Sci U S A 2004;101:7885–90. [PubMed: 15143215]
32. Kamen DE, Griko Y, Woody RW. The stability, structural organization, and denaturation of pectate lyase C, a parallel beta-helix protein. Biochemistry 2000;39:15932–43. [PubMed: 11123920]
33. Santoso A, Chien P, Osherovich LZ, Weissman JS. Molecular basis of a yeast prion species barrier. Cell 2000;100:277–88. [PubMed: 10660050]
34. Chien P, DePace AH, Collins SR, Weissman JS. Generation of prion transmission barriers by mutational control of amyloid conformations. Nature 2003;424:948–51. [PubMed: 12931190]
35. Bradley ME, Edskes HK, Hong JY, Wickner RB, Liebman SW. Interactions among prions and prion "strains" in yeast. Proc Natl Acad Sci U S A 2002;99 (Suppl 4):16392–9. [PubMed: 12149514]
36. Derkatch IL, et al. Effects of Q/N-rich, polyQ, and non-polyQ amyloids on the de novo formation of the [PSI+] prion in yeast and aggregation of Sup35 in vitro. Proc Natl Acad Sci U S A 2004;101:12934–9. [PubMed: 15326312]
37. Nakayashiki T, Ebihara K, Bannai H, Nakamura Y. Yeast [PSI+] "prions" that are crosstransmissible and susceptible beyond a species barrier through a quasi-prion state. Mol Cell 2001;7:1121–30. [PubMed: 11430816]
38. Liu JJ, Lindquist S. Oligopeptide-repeat expansions modulate 'protein-only' inheritance in yeast. Nature 1999;400:573–6. [PubMed: 10448860]
39. Parham SN, Resende CG, Tuite MF. Oligopeptide repeats in the yeast protein Sup35p stabilize intermolecular prion interactions. Embo J 2001;20:2111–9. [PubMed: 11331577]
40. Osherovich LZ, Cox BS, Tuite MF, Weissman JS. Dissection and design of yeast prions. PLoS Biol 2004;2:E86. [PubMed: 15045026]

41. Balbirnie M, Grothe R, Eisenberg DS. An amyloid-forming peptide from the yeast prion Sup35 reveals a dehydrated beta-sheet structure for amyloid. Proc Natl Acad Sci U S A 2001;98:2375–80. [PubMed: 11226247]

42. Bradley ME, Liebman SW. The Sup35 domains required for maintenance of weak, strong or undifferentiated yeast [PSI+] prions. Mol Microbiol 2004;51:1649–59. [PubMed: 15009892]

43. Eakin CM, Attenello FJ, Morgan CJ, Miranker AD. Oligomeric assembly of native-like precursors precedes amyloid formation by beta-2 microglobulin. Biochemistry 2004;43:7808–15. [PubMed: 15196023]

44. Hwang W, Zhang S, Kamm RD, Karplus M. Kinetic control of dimer structure formation in amyloid fibrillogenesis. Proc Natl Acad Sci U S A 2004;101:12916–21. [PubMed: 15326301]

45. Lee S, Eisenberg D. Seeded conversion of recombinant prion protein to a disulfide-bonded oligomer by a reduction-oxidation process. Nat Struct Biol 2003;10:725–30. [PubMed: 12897768]

46. Garzon-Rodriguez W, et al. A conformation change in the carboxyl terminus of Alzheimer's Abeta (1–40) accompanies the transition from dimer to fibril as revealed by fluorescence quenching analysis. J Biol Chem 2000;275:22645–9. [PubMed: 10806193]

47. Barghorn S, Mandelkow E. Toward a unified scheme for the aggregation of tau into Alzheimer paired helical filaments. Biochemistry 2002;41:14885–96. [PubMed: 12475237]

48. Wille H, et al. Structural studies of the scrapie prion protein by electron crystallography. Proc Natl Acad Sci U S A 2002;99:3563–8. [PubMed: 11891310]

49. Govaerts C, Wille H, Prusiner SB, Cohen FE. Evidence for assembly of prions with left-handed beta-helices into trimers. Proc Natl Acad Sci U S A 2004;101:8342–7. [PubMed: 15155909]

50. Safar J, et al. Eight prion strains have PrP(Sc) molecules with different conformations. Nat Med 1998;4:1157–65. [PubMed: 9771749]

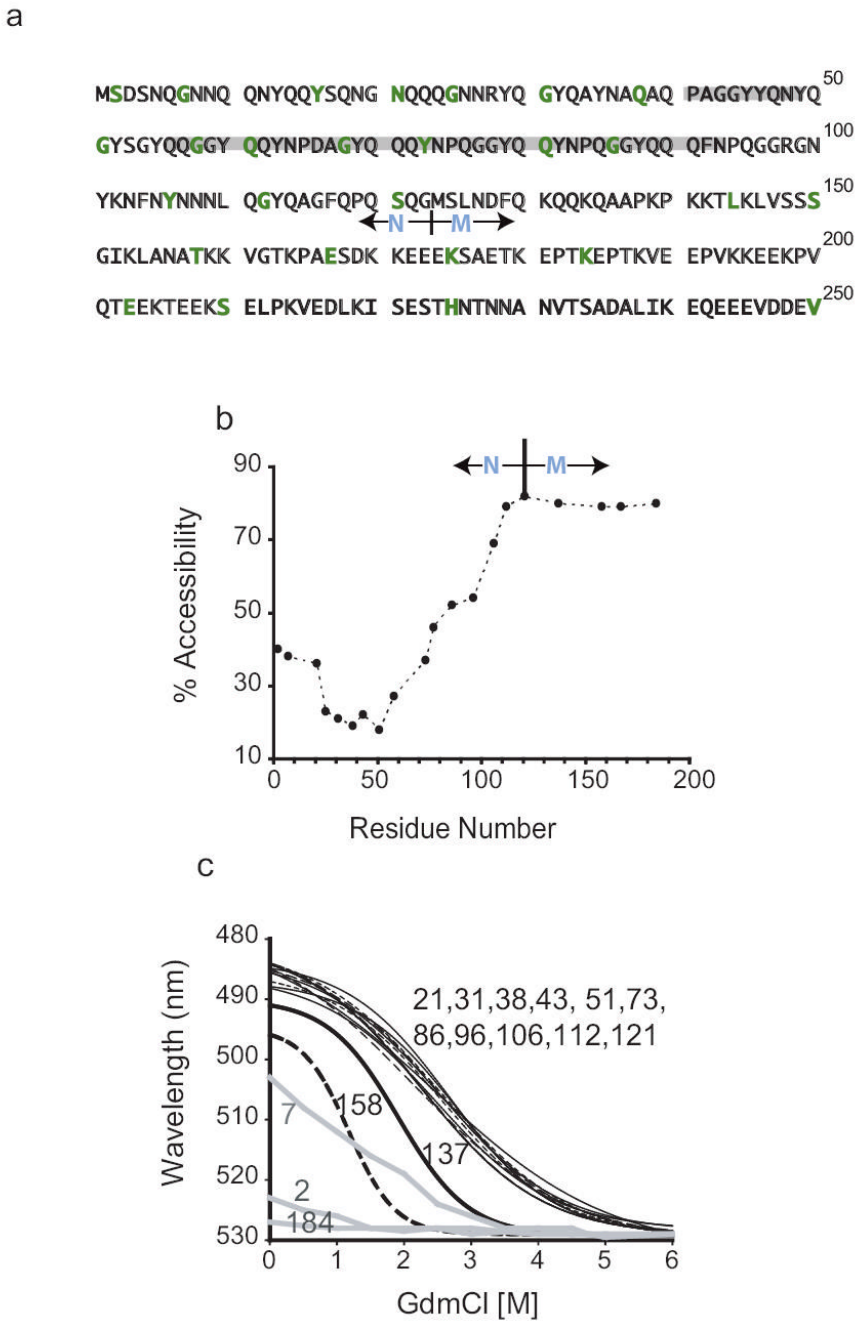

Figure 1. Mapping the amyloid region of NM fibres.

(a) NM sequence, showing residues mutated to cysteine in green, the five imperfect oligopeptide repeats shaded in grey, and the boundary between N and M as it is traditionally drawn. By aa composition, the boundary might equally well be drawn at aa 138.

(b) Accessibility of cysteine residues after assembly. Fibres, formed from single cysteine substitution mutants were labelled with pyrene maleimide for 3 hours. The ratio of labelled/unlabelled protein is plotted as a measure of accessibility. For all proteins labelling approached 100% in denaturant (6M GdmCl; data not shown),

(c) Denaturation profiles. Mutants were individually assembled at 25°C, using 75% unlabelled and 25% acrylodan-labelled protein. Each preparation was then equilibrated for 30 minutes at 24 different concentrations of GdmCl and fluorescence spectra were recorded.

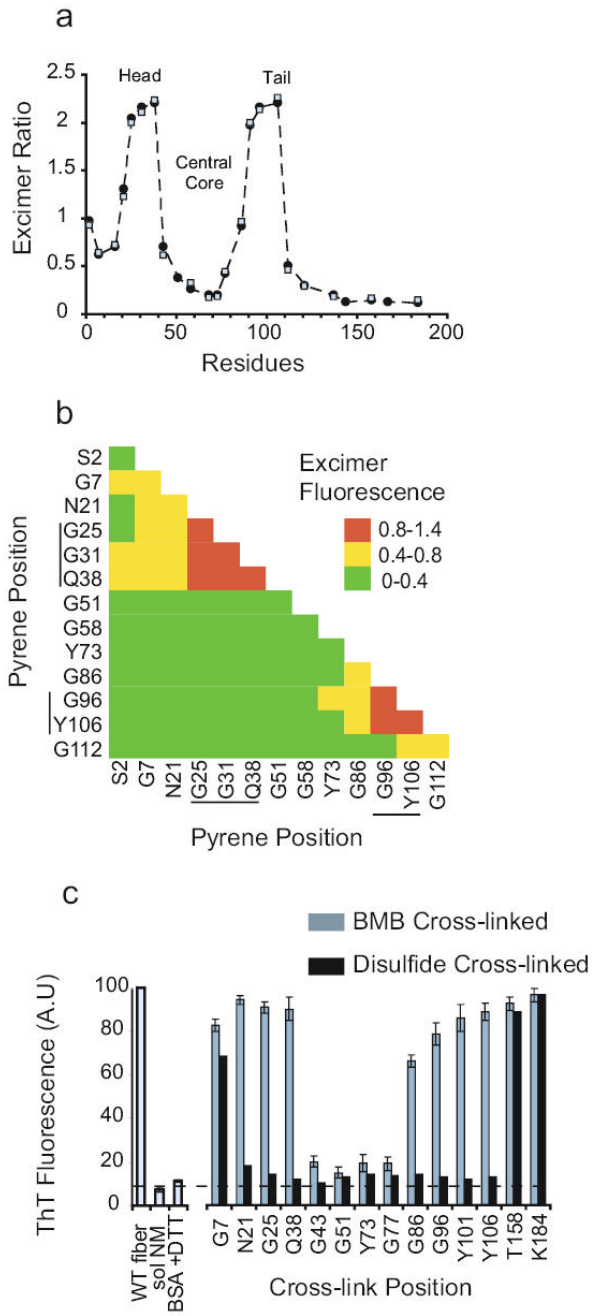

Figure 2. Intermolecular contacts in NM fibres.

(a) Proximity analysis assessed by excimer fluorescence in fibres carrying pyrene labels at single sites. Fibres were assembled at 25°C with 2.5μM NM (60 % labelled), either by gently rotating the samples (•), or by adding 4% sonicated seed (▒) formed at 25°C. The ratio of excimer fluorescence/non-excimer fluorescence (I_{465}/I_{375}) is plotted.

(b) Excimer fluorescence in fibres assembled from mixtures of two different pyrene-labelled cysteine variants. Fibres were assembled at 25°C with gentle rotation, in reactions containing equimolar mixtures of each variant (25 % labelled and 75% unlabelled). Actual excimer values are provided in Fig. S3. Head and Tail region residues are marked.

(c) Effects of cross-links on amyloid assembly. Right, proteins cross-linked under denaturing conditions with either a 2Å disulfide bond (black bars) or a flexible 11Å BMB cross-link (grey bars) were diluted 200 fold into buffer to a final concentration of 2.5μM NM and assembled with rotation at 25°C. Left, thioflavinT, ThT, values for WT fibres, soluble NM, and a denatured standard (bovine serum albumin treated with DTT to induce denaturation). Values represent means ± SD (n=3 experiments)

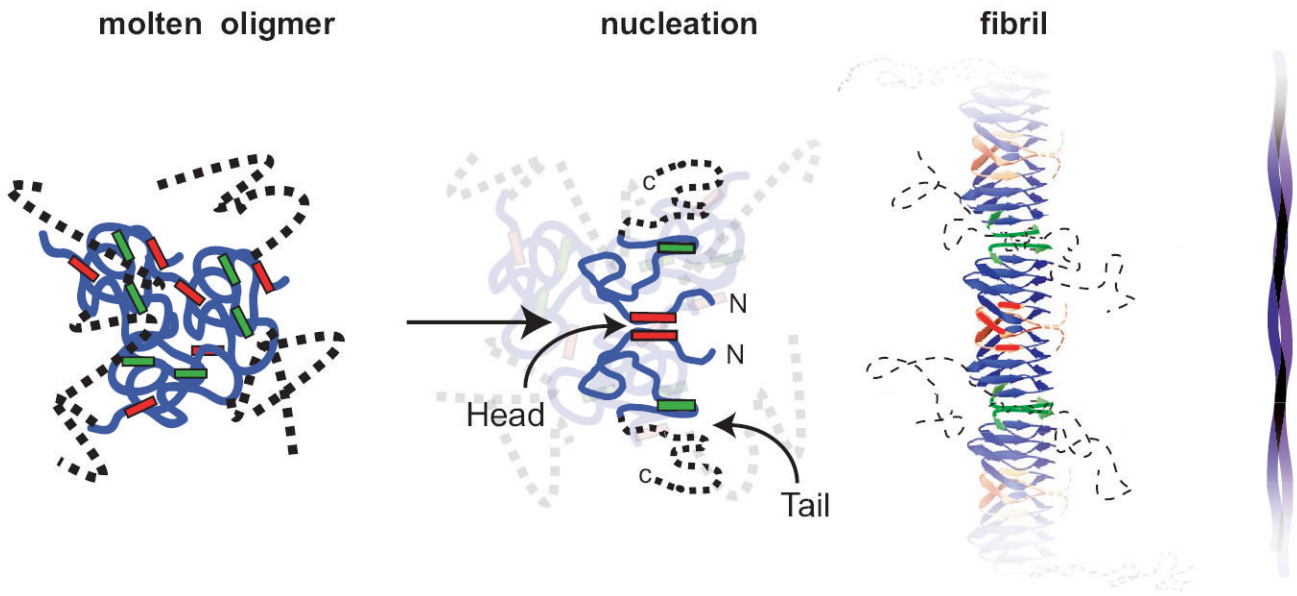

Figure 3. An example of NM assembly that conforms to our data.

One model for NM assembly is provided to illustrate the constraints that our data place on the nature of NM fibre structures. In the cooperatively folded amyloid core, Head residues in one NM molecule are in close proximity to Head residues of their neighbours; the same is true for the Tail (3). Central Core residues are sequestered from intermolecular interactions. M is largely unstructured, but the segment of M proximal to N becomes structured when amyloid forms. In the initial stages, NM molecules rapidly acquire a collapsed state (1) that retains a molten character until the Head regions of two molecules (2) come into proximity with each other and nucleate assembly. We do not know how fibrils are arranged within fibres (4).

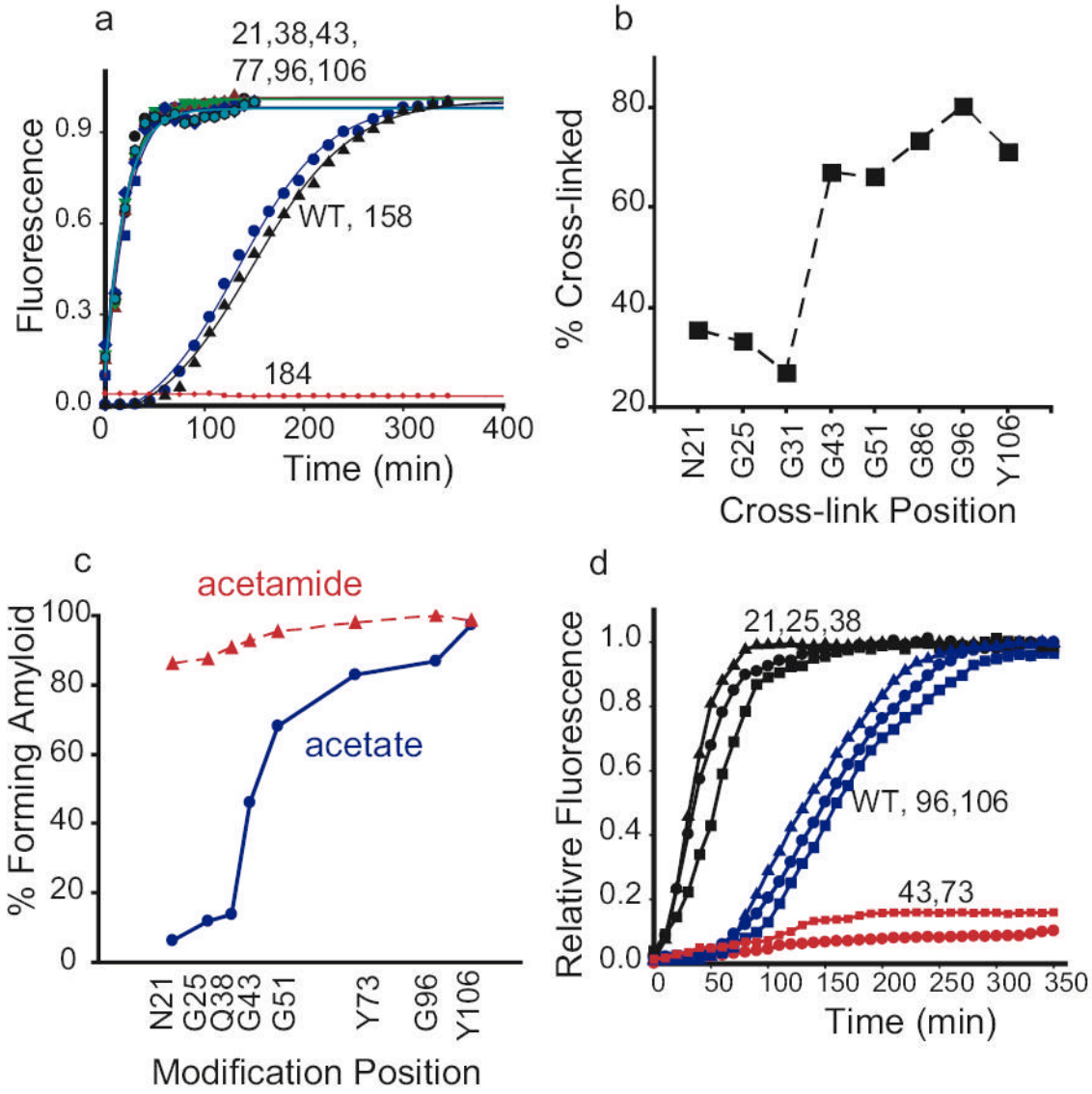

Figure 4. Early assembly events.

a) Formation of a collapsed intermediate: An increase in acrylodan fluorescence at positions N21 (■), Q38 (■), G43 (▲), Y77 (▼), G96 (⬟), Y106 (◆) occurred very rapidly after proteins were diluted into buffer, before the formation of amyloid (also see Fig. S4). Amyloid formation was assessed by SDS insolubility because acrylodan and ThT fluorescence could not be analysed in the same reaction. Acrylodan fluorescence for mutants T158C (▲) and K184C (●) in the M domain and ThT binding profiles of WT NM (●) are plotted for comparison.

(b) Susceptibility of different cysteines to spontaneous cross-linking during assembly under non-reducing conditions. Crosslinks were assessed by non-reducing SDS-PAGE.

(c) Addition of a single charge in the Head region severely impedes fibre assembly. Assembly of negatively charged iodoacetate (●) and uncharged iodoacetamide (▲) labelled proteins was monitored by ThT fluorescence.

(d) Assembly kinetics of cysteine variants cross-linked with BMB at position N21C (▲), G25C (•), Q38C (▪), Wt NM (▲), G96 (●), Y106C (■) and G43C (■) and Y73C (●) monitored by ThT fluorescence.

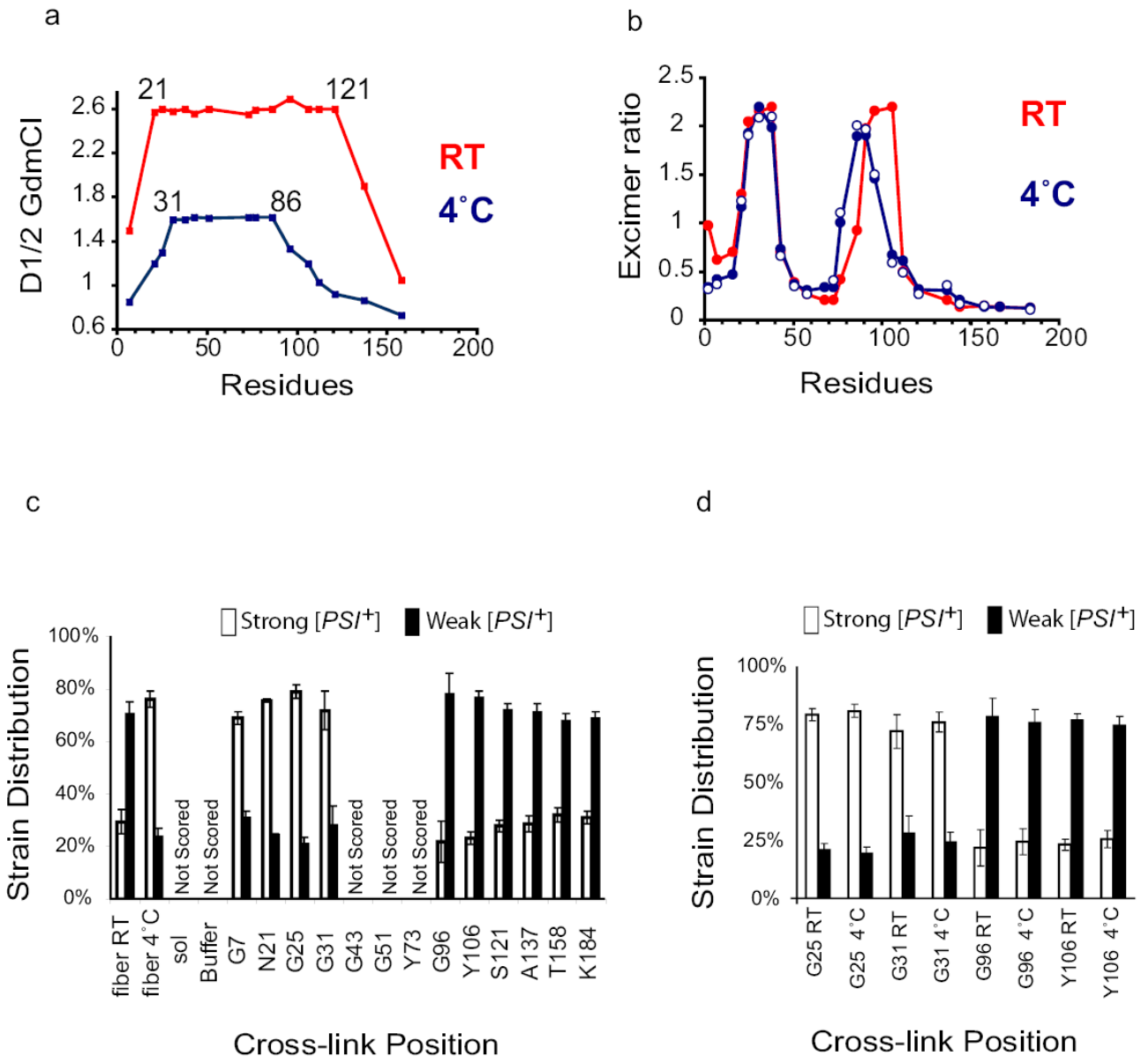

Figure 5. Structural distinctions between prion strain populations

a) Amyloid core length and stability differ in fibres assembled at 4°C and 25°C. Acrylodan-labelled fibres assembled at 4°C (■) and 25°C (■) were denatured as in Fig. 1b. $D_{1/2}$ values were obtained from full GdmCl denaturation profiles (see Fig 1c).

(b) Intersubunit interfaces change in fibres assembled at different temperatures. Excimer fluorescence of pyrene-labelled mutants assembled in rotated unseeded reactions at 25°C (●), 4°C (●) or in seeded unrotated reactions with 4% seed formed at 4°C (⊖). Pyrene fluorescence is similar in seeded and unseeded reactions.

(c) BMB cross-links at different positions bias assembly towards distinct prion strains. NM proteins cross-linked in denaturant were diluted into buffer, assembled into fibres, and used to transform [*psi*$^-$] cells to [*PSI*$^+$] state. Left, controls: uncross-linked WT fibres assembled at RT or at 4°C are biased towards the production of weak or strong strains, respectively[27].

Soluble NM, buffer alone, and proteins cross-linked in the Central Core did not induce [*PSI*$^+$] above background and were not scored. Values represent means ± SD (n=5 experiments) (d) Strain biases created by cross-linking overcome the biases created by assembly at different temperatures. Whether they were assembled at 4°C or at RT, fibres cross-linked in the Head (G25C or G31C) produced mostly strong [*PSI*$^+$] strains, and fibres cross-linked in the Tail (G96C and106C) produced mostly weak [*PSI*$^+$] strains. Values represent means ± SD (n=5 experiments)